



**HAL**  
open science

# Biochemical characterization and mutational studies of the thermostable uracil DNA glycosylase from the hyperthermophilic euryarchaeon *Thermococcus barophilus* Ch5

Haoqiang Shi, Qi Gan, Donghao Jiang, Yuqi Wu, Youcheng Yin, Haiyue Hou, Hongxun Chen, Li Miao, Zhihui Yang, Phil M. Oger, et al.

## ► To cite this version:

Haoqiang Shi, Qi Gan, Donghao Jiang, Yuqi Wu, Youcheng Yin, et al.. Biochemical characterization and mutational studies of the thermostable uracil DNA glycosylase from the hyperthermophilic euryarchaeon *Thermococcus barophilus* Ch5. *International Journal of Biological Macromolecules*, 2019, 10.1016/j.ijbiomac.2019.05.073 . hal-02130096

**HAL Id: hal-02130096**

**<https://hal.science/hal-02130096v1>**

Submitted on 4 Nov 2020

**HAL** is a multi-disciplinary open access archive for the deposit and dissemination of scientific research documents, whether they are published or not. The documents may come from teaching and research institutions in France or abroad, or from public or private research centers.

L'archive ouverte pluridisciplinaire **HAL**, est destinée au dépôt et à la diffusion de documents scientifiques de niveau recherche, publiés ou non, émanant des établissements d'enseignement et de recherche français ou étrangers, des laboratoires publics ou privés.

1  
2  
3  
4 **Biochemical characterization and mutational studies of the thermostable uracil**  
5  
6 **DNA glycosylase from the hyperthermophilic euryarchaeon *Thermococcus***  
7 ***barophilus* Ch5**  
8  
9

10  
11  
12  
13  
14  
15  
16 Haoqiang Shi<sup>a</sup>, Qi Gan<sup>a</sup>, Haiyue Hou<sup>a</sup>, Hongxun Chen<sup>a</sup>, Yinuo Xu<sup>a</sup>, Li Miao<sup>a</sup>, Zhihui

17  
18 Yang<sup>b#</sup>, Philippe Oger<sup>c#</sup> and Likui Zhang<sup>a#</sup>  
19  
20  
21  
22

23 <sup>a</sup>Marine Science & Technology Institute

24  
25 Department of Environmental Science and Engineering, Yangzhou University, China  
26

27 <sup>b</sup>College of Plant Protection, Agricultural University of Hebei, Baoding City, Hebei

28  
29 Province 071001, China  
30  
31

32 <sup>c</sup>Université de Lyon, INSA de Lyon, CNRS UMR 5240, Lyon, France  
33  
34

35 Corresponding author: Dr. Likui Zhang  
36

37 E-mail address: [lkzhang@yzu.edu.cn](mailto:lkzhang@yzu.edu.cn)  
38

39 Tel: +86-514-89795882  
40

41 Fax: +86-514-87357891  
42  
43

44 Corresponding author: Prof. Zhihui Yang  
45

46 E-mail address: [bdybh@hebau.edu.cn](mailto:bdybh@hebau.edu.cn)  
47  
48

49 Corresponding author: Prof. Philippe Oger  
50

51 E-mail address: [philippe.oger@insa-lyon.fr](mailto:philippe.oger@insa-lyon.fr)  
52  
53  
54  
55  
56  
57  
58  
59

60  
61  
62  
63 **Abstract**  
64

65 Uracil DNA glycosylases (UDGs) play an important role in removing uracil from  
66 DNA to initiate DNA base excision repair. Here, we first characterized biochemically  
67 a thermostable UDG from the hyperthermophilic euryarchaeon *Thermococcus*  
68 *barophilus* Ch5 (Tba UDG), and probed its mechanism by mutational analysis.  
69  
70 The recombinant Tba UDG cleaves specifically uracil-containing ssDNA and dsDNA  
71 at 65°C. The enzyme displays an optimal cleavage activity at 55–75°C. Tba UDG  
72  
73 cleaves DNA over a wide pH spectrum ranging from 4.0 to 9.0 with an optimal pH of  
74  
75 5.0–8.0. In addition, the Tba UDG activity is independent on a divalent metal ion;  
76  
77 however, both Zn<sup>2+</sup> and Cu<sup>2+</sup> completely inhibits the enzyme activity. Furthermore,  
78  
79 the Tba UDG activity is also inhibited by high NaCl concentration. Tba UDG  
80  
81 removes uracil from DNA by the order: U≈U/G>U/T≈U/C>U/A. The mutational  
82  
83 studies showed that both the E118A and N159A mutants completely abolish the  
84  
85 cleavage activity and retain the compromised binding activity, suggesting that  
86  
87 residues E118 and N159 in Tba UDG are important for uracil recognition and removal.  
88  
89 Our work provides a basis for determining the role of Tba UDG in the base excision  
90  
91 repair pathway for uracil repair in *Thermococcus*.  
92  
93  
94  
95  
96  
97  
98  
99  
100  
101  
102

103 **Keywords:** *Thermococcus barophilus*; Uracil DNA glycosylase; Base excision  
104  
105 repair  
106  
107  
108  
109  
110  
111  
112  
113  
114  
115  
116  
117  
118

## 1. Introduction

Uracil bases in DNA are created by deamination of cytosine or by dUMP incorporation catalyzed by a DNA polymerase. It is estimated that the deamination of cytosine leads to up to 500 uracil residues in a single human cell each day [1-2]. The rate of deamination of cytosine is greatly enhanced at elevated temperatures [3], and thus hyperthermophilic organisms that live at temperatures above 80°C are facing a serious threat caused by cytosine deamination. Since uracil has a strong ability to form mismatch with adenine (A), a G-C base pair would be subsequently converted to an A-T base pair if DNA replication occurs before the uracil is repaired [4], potentially leading to mutations in the genome. However, the estimated spontaneous mutation rates in hyperthermophilic bacteria and archaea are similar to those observed in *Escherichia coli* [5-6], suggesting that hyperthermophilic microorganisms are more efficient in repairing hydrolytic and oxidative damage to DNA bases [7]. Increased GC to AT mutations by replicating uracil that originates from deamination of cytosine are detrimental to the cells, which may cause genome instability or even cancer occurrence. In response, cells have evolved a base excision repair (BER) pathway to counteract potential mutations generated by uracil replication. Uracil DNA glycosylase (UDG) is the first BER enzyme to remove uracil from DNA, which leads to apurinic/apyrimidinic (AP) site. The generated AP site is subsequently repaired by different enzymes: AP endonuclease, DNA deoxyribosephosphodiesterase, DNA polymerase and DNA ligase [8].

UDGs are ubiquitous in bacteria, archaea, eukarya and viruses, and can remove

178  
179  
180  
181 uracil from DNA through hydrolyzing their glycosyl bonds. Based on sequence  
182  
183 similarity, UDGs have currently been classified into six families [9]. Family 1 UDGs  
184  
185 have been well studied in *Escherichia coli* and human [10-15], and can remove uracil  
186  
187 base efficiently from ssDNA and from ds DNA. Mismatch-specific DNA glycosylases  
188  
189 and single-stranded specific monofunctional UDGs form families 2 and 3,  
190  
191 respectively [16-17]. Family 4 UDGs are exclusively observed in the  
192  
193 hyperthermophilic microorganisms and possess a 4Fe - 4S cluster [18-20]. Family 5  
194  
195 UDGs have broad substrate specificity, but lack a polar residue at the active-site motif  
196  
197 [20, 21-22]. Last, family 6 UDGs can cleave hypoxanthine instead of uracil, and  
198  
199 thus belong to hypoxanthine DNA glycosylase family [23].  
200  
201  
202  
203  
204

205 The *Archaeoglobus fulgidus* UDG is the first enzyme to be identified and  
206  
207 characterized from archaea [24]. Currently, another eight UDG homologues from  
208  
209 hyperthermophilic archaea have been reported from *Pyrobaculum aerophilum* [25],  
210  
211 *Pyrococcus furiosus* [26-27], *Methanococcus jannaschii* [28], *Aeropyrum pernix* [29],  
212  
213 *Sulfolobus solfataricus* [30], *Sulfolobus tokodaii* [31-32], *Sulfolobus acidocaldarius*  
214  
215 [33], and *Thermoplasma acidophilum* [34]. The *A. fulgidus* UDG is the most  
216  
217 thermostable, retaining activity even after 1.5 hr of heating at 95°C [24]. It is able to  
218  
219 remove uracil from dsDNA containing a U/A or U/G base pair, as well as from  
220  
221 ssDNA. This enzyme is inhibited by apurinic sites. *M. jannaschii* UDG possesses the  
222  
223 helix-hairpin-helix and [4Fe-4S]-binding cluster to recognize and bind uracil, and can  
224  
225 efficiently cleave uracil in ssDNA and dsDNA and 8-oxoG in DNA [28]. The crystal  
226  
227 structure of *S. tokodaii* UDG shows that residues Leu169, Tyr170 and Asn171 in the  
228  
229  
230  
231  
232  
233  
234  
235  
236

237  
238  
239  
240 leucine-intercalation loop of the enzyme play important roles in uracil-binding [32]. *T.*  
241  
242 *acidophilum* UDG is involved in mediating the transfer from long patch repair to short  
243  
244 patch repair [34]. Several studies on archaeal UDGs have shown that they can interact  
245  
246 with PCNA (proliferating cell nuclear antigen) [26, 30, 35], which is an important  
247  
248 component in DNA replication and repair in and eukarya and archaea [36].  
249  
250 Furthermore, due to their thermostability, they have been shown to have potential  
251  
252 applications to enhance PCR yield or to help in jump starting the reactions [29].  
253  
254  
255  
256

257 *Thermococcus* is an important branch of euryarchaea comprising more than 40  
258  
259 described species, which mostly thrive in the hottest deep-sea hydrothermal vent  
260  
261 systems. Thus, similar to other hyperthermophilic archaea and bacteria,  
262  
263 *Thermococcus* is also facing severe challenges due to increased deamination of  
264  
265 cytosine dependent on high-temperature [37]. It is expected that the  
266  
267 hyperthermophilic *Thermococcus* would have evolved a repair pathway to counteract  
268  
269 the mutational effects of cytosine deamination in order to maintain their genome  
270  
271 stability. *Thermococcus barophilus* is one of the most extreme member of the  
272  
273 *Thermococcus* genus, being hyperthermophilic, piezophilic and capable of  
274  
275 auxotrophic growth on carbon monoxide. Strain Ch5 was isolated from a deep-sea  
276  
277 hydrothermal field of the Mid-Atlantic Ridge (Logachev field chimney, 3,020 m  
278  
279 depth) [38]. *T. barophilus* Ch5 has a pressure optimum of 40 MPa and a temperature  
280  
281 optimum of 85°C [39]. The completed genome sequence of *T. barophilus* Ch5 shows  
282  
283 that this strain possesses two uracil DNA glycosylases (Tba UDGs) [40]. In this study,  
284  
285 we cloned one of the Tba UDGs gene, purified and characterized its product. In  
286  
287  
288  
289  
290  
291  
292  
293  
294  
295

296  
297  
298  
299 addition, we probed the mechanism of cleaving uracil by Tba UDG through  
300  
301 mutational analysis. We report here that Tba UDG is a thermostable enzyme cleaving  
302  
303 specifically uracil-containing DNA, and its residues E118 and N159 are important for  
304  
305 its catalysis. To the best of our knowledge, this is the first report of the biochemical  
306  
307 characterization and mutational studies of a thermostable UDG from *Thermococcus*  
308  
309 species.  
310  
311  
312

## 313 **2. Materials and methods**

### 314 *2.1. Cloning, expression and purification of Tba UDG*

315  
316 The Tba UDG in this work is encoded by gene TBCH5v1\_0629 (GenBank  
317  
318 accession number: CP013050.1). The genomic DNA of *T. barophilus* Ch5 was  
319  
320 extracted as described by Oger et al. [40] and then used as a template to amplify the  
321  
322 gene TBCH5v1\_0629 using the Phusion DNA polymerase (Thermo Scientific,  
323  
324 Waltham, MA, USA) and the two primers (Tba UDG F and Tba UDG R, Table 1).  
325  
326 The amplified DNA product was inserted into the vector pET-30a (+) (Novagen,  
327  
328 Merck, Darmstadt, Germany). The recombinant plasmid harboring a sequence  
329  
330 encoded a 6 × His-tag at the C-terminus of Tba UDG was sequenced to verify the  
331  
332 accuracy of the sequence of the enzyme gene and transformed into *E. coli* BL21  
333  
334 (DE3) cells (Transgene, Beijing, China) for protein expression.  
335  
336  
337  
338  
339  
340  
341

342 The expression strain *E. coli* harboring the recombinant plasmid was cultured  
343  
344 into LB medium with 100 µg/mL kanamycin at 37°C until an OD<sub>600</sub> of 0.6, at which  
345  
346 point protein expression was induced with isopropyl thiogalactoside (IPTG) at a final  
347  
348 concentration of 0.1 mM. The culture was further shaken for 10 hr at room  
349  
350  
351  
352  
353  
354

355  
356  
357  
358 temperature until it reached an OD<sub>600</sub> of 1.1.  
359

360 The cells were harvested by centrifugation (5,000 × g for 20 min at room  
361 temperature). The resultant pellet was resuspended with Ni column buffer A (20 mM  
362 Tris-HCl pH 8.0, 1 mM dithiothreitol (DTT), 500 mM NaCl, 50 mM imidazole and  
363 10% glycerol). The cells were disrupted by sonication into an ice bath. After  
364 centrifugation (16,000 × g for 30 min at 4°C), the supernatant was collected into a 50  
365 mL tube and heated at 70°C for 20 min. The non-thermostable *E. coli* proteins were  
366 almost removed by centrifugation (16,000 × g for 30 min at 4°C). The resulting  
367 supernatant was loaded to a HisTrap FF column (GE Healthcare, Uppsala, Sweden)  
368 and purified with NCG™ Chromatography System (Bio-Rad, Hercules, CA, USA). A  
369 linear gradient of 50–500 mM imidazole was used to elute the Tba UDG protein.  
370 Fractions of Tba UDG protein were harvested and run by a 12% sodium dodecyl  
371 sulfate-polyacrylamide gel electrophoresis. The Tba UDG protein was stained and  
372 visualized by Coomassie-staining method. Finally, the purified Tba UDG protein was  
373 dialyzed in a storage buffer containing 50 mM Tris-HCl pH 8.0, 50 mM NaCl, 1 mM  
374 DTT and 50% glycerol, and was stored at –80°C. The protein concentration was  
375 determined using the Bradford Protein Assay Kit (Bio-Rad).  
376  
377  
378  
379  
380  
381  
382  
383  
384  
385  
386  
387  
388  
389  
390  
391  
392  
393  
394  
395  
396  
397

## 398 2.2. Construction, overexpression and purification of the Tba UDG mutants 399 400

401 Using the wild-type plasmid harboring the Tba UDG gene as a template, the site-  
402 directed mutagenesis was performed by a SDM Kit to construct E118A and N159A  
403 mutants, according to its manual instruction. Note that residues E118 and N159 in Tba  
404 UDG are located in the conserved Motif B and Motif D, respectively (Fig. 1). The  
405  
406  
407  
408  
409  
410  
411  
412  
413



414 sequences of mutagenic primers are listed in Table 1. The mutant plasmids were  
415  
416  
417  
418  
419  
420  
421  
422  
423  
424  
425  
426  
427  
428  
429  
430  
431  
432  
433  
434  
435  
436  
437  
438  
439  
440  
441  
442  
443  
444  
445  
446  
447  
448  
449  
450  
451  
452  
453  
454  
455  
456  
457  
458  
459  
460  
461  
462  
463  
464  
465  
466  
467  
468  
469  
470  
471  
472

sequences of mutagenic primers are listed in Table 1. The mutant plasmids were verified by sequencing. Similar to the wild-type protein, the Tba UDG mutant proteins were overexpressed, purified and quantitated.

### 2.3. DNA substrate

Normal and uracil-containing deoxyoligonucleotides were synthesized by Sangon Biotech company, China. The sequences of these deoxyoligonucleotides are shown in Table 2. The Cy3-labeled deoxyoligonucleotide duplexes shown in Table 3 were prepared by annealing the Cy3-labeled deoxyoligonucleotides to the complementary deoxyoligonucleotides in a buffer containing 20 mM Tris-Cl pH 8.0 and 100 mM NaCl. The mixture was heated at 100°C for 5 min and cooled slowly at least 4 hours to room temperature.

### 2.4. Glycosylase assays

The standard assays of Tba UDG activity were carried out in the reactions (10  $\mu$ L) which contained 20 mM Tris-HCl pH 8.0, 5 mM DTT, 50 mM NaCl, 1 mM EDTA, 8% glycerol, 200 nM DNA, wild-type or mutant Tba UDG with varied concentrations. The reactions were performed at 75°C for 10 min for ssDNA cleavage and at 65°C for 10 min for dsDNA cleavage. 1  $\mu$ L 500 mM NaOH and 9  $\mu$ L formamide-EDTA (98% formamide and 20 mM EDTA) were added to stop the reactions. The reaction products were heated at 95°C for 5 min and chilled rapidly on ice for 5 min, and then loaded onto a denaturing 15% polyacrylamide gel with 8M urea. After electrophoresis, the gels were scanned and the Cy3-labeled DNA was visualized with a Molecular Image analyser (PharosFx System, Bio-Rad). The

473  
474  
475  
476 ImageQuant software was used for the quantitative analysis. All experiments of the  
477  
478 glycosylase assays were replicated three times.  
479  
480

#### 481 *2.5. Biochemical characterization assays*

482

483 The optimal temperature of Tba UDG to cleave DNA in the reactions (10  $\mu$ L)  
484 contained 800 nM enzyme and 200 nM Cy3-labeled ssDNA with uracil as a target.  
485  
486 The reactions were performed at 35, 45, 55, 65, 75, 85 and 95°C for uracil-containing  
487  
488 ssDNA for 10 min.  
489  
490

491  
492 To examine the thermostability of the enzyme, Tba UDG was heated at 80, 85,  
493  
494 90, 95 and 100°C for 30 min. The activity of the heated Tba UDG protein were  
495  
496 investigated under the same conditions but using 1  $\mu$ M of the heated enzyme protein.  
497  
498 Samples were treated as described above.  
499  
500

501  
502 The effect of pH on the Tba UDG activity was evaluated by examining DNA  
503  
504 cleavage in similar 10  $\mu$ L reactions at 75°C under pHs ranging from 4.0 to 11.0 using  
505  
506 1  $\mu$ M of the enzyme protein. The varied pHs were adjusted with five different buffers  
507  
508 (all at 20 mM concentrations): acetate-sodium acetate (pH 4.0 and pH 5.0), sodium  
509  
510 phosphate-NaOH (pH 6.0 and pH 7.0), Tris-HCl (pH 8.0), Gly-NaOH (pH 9.0), and  
511  
512 NaHCO<sub>3</sub>-NaOH (pH 10.0 and pH 11.0).  
513  
514  
515

516  
517 The effect of divalent metal ions on Tba UDG activity was investigated by  
518  
519 adding of 2 mM of Mg<sup>2+</sup>, Mn<sup>2+</sup>, Ca<sup>2+</sup>, Zn<sup>2+</sup> or Cu<sup>2+</sup> (analytical purity) to the reaction  
520  
521 mixture. Assays were performed at 75°C with 250 nM of the enzyme. Samples were  
522  
523 treated as described above.  
524  
525

526 To evaluate the effect of salinity on Tba UDG activity, glycosylase assays were  
527  
528  
529  
530  
531

532  
533  
534  
535 performed in the presence of various NaCl concentrations ranging from 50 to 1,000  
536 mM using 1  $\mu$ M of the enzyme. Samples were treated as described above.  
537  
538

#### 539 540 2.6. *Glycosylase single-turnover assays* 541

542 The reaction mixtures containing 800 nM wild-type or mutant Tba UDG and 200  
543 nM DNA substrates were incubated at 65°C for various times. Samples were treated  
544 as described above. Data from the DNA cleavage experiments under single-turnover  
545 conditions were fit to a single-exponential decay equation:  
546  
547  
548  
549

$$550 \quad [\text{Product}] = A \exp(-k_{\text{endo}} t)$$

551  
552 where  $A$  and  $k_{\text{endo}}$  represent the reaction amplitude and observed DNA cleavage  
553 rate, respectively.  
554  
555  
556

#### 557 558 2.7. *Substrate specificity* 559

560  
561 To investigate the substrate specificity of the enzyme, we employed normal  
562 ssDNA and dsDNA, ssDNA with uracil and dsDNA with U (U/T, U/C, U/G or U/A),  
563 and dsDNA with a mismatch (G/T) as the substrates to perform the glycosylase assays  
564 at 65°C for 10 min using 800 nM enzyme. Samples were treated as described above.  
565  
566  
567  
568

#### 569 570 2.8. *DNA-binding Assays* 571

572  
573 Electrophoresis mobility shift assays (EMSA) were performed by incubating the  
574 wild-type or mutant Tba UDG with uracil-containing ssDNA and dsDNA in a DNA  
575 binding buffer (10  $\mu$ L) containing 20 mM Tris-HCl pH 8.0, 5 mM DTT, 8% glycerol,  
576 200 nM DNA and the wild-type or mutant Tba UDG with varied concentrations at  
577 25°C for 10 min. The samples were electrophoresed on a 4% native polyacrylamide  
578 gel in 0.1  $\times$  TBE (Tris-borate-EDTA) buffer. After electrophoresis, the gels were  
579  
580  
581  
582  
583  
584  
585  
586  
587  
588  
589  
590

591 scanned and Cy3-labeled DNA was visualized with a Molecular Image analyser (Bio-  
592 Rad). ImageQuant software was used for the quantitative analysis.  
593  
594  
595  
596  
597

### 598 **3. Results**

#### 600 *3.1. Tba UDG is a thermostable uracil DNA glycosylase*

601  
602 The alignment result of partial amino acid sequences of UDGs from  
603 hyperthermophilic archaea and bacteria shows that Tba UDG possesses six conserved  
604 motifs (A-F) that are characteristics of family 4 UDGs (Fig. 1A), suggesting that this  
605 enzyme belongs to family 4 UDGs. On the other hand, Motif B and Motif F in Tba  
606 UDG are conserved in all six family UDGs (Fig. 1B). Tba UDG displays 21%, 19%,  
607 22%, 22%, 18%, 20%, 19%, and 21% similarities to those of from *P. furiosus*, *P.*  
608 *horikoshii*, *A. fulgidus*, *P. aerophilum* UDGA, *A. pernix*, *S. solfataricus*, *S. tokodaii*  
609 and *Thermotoga maritima*, respectively. The low similarity between Tba UDG and  
610 other UDGs suggests that Tba UDG might be a novel glycosylase.  
611  
612  
613  
614  
615  
616  
617  
618  
619  
620  
621  
622  
623  
624

625 The Tba UDG gene from the hyperthermophilic archaeon *T. barophilus* Ch5 was  
626 cloned into the pET-30a (+) expression vector, and expressed in *E. coli* BL21(DE3).  
627 The recombinant Tba UDG protein was successfully expressed as a His-tag fusion  
628 protein (Fig. 1C). By means of sonication, heat treatment (70°C for 20 min) and  
629 purification by affinity chromatography with a Ni column, we purified the Tba UDG  
630 protein (~27 kDa) (Fig. 1C).  
631  
632  
633  
634  
635  
636  
637  
638

639 We used the normal, uracil-containing ssDNA and dsDNA as the substrates to  
640 investigate DNA cleavage by Tba UDG at 65°C. Using normal ssDNA and dsDNA as  
641 the substrates, no product was formed by the enzyme, however, the cleaved product of  
642  
643  
644  
645  
646  
647  
648  
649

650  
651  
652  
653 the enzyme was observed in the presence of uracil-containing ssDNA and dsDNA  
654  
655 (Fig. 1D). The results showed that Tba UDG is a thermostable glycosylase, capable of  
656  
657 removing uracil from ssDNA and dsDNA at 65°C.  
658

659  
660 The heating treatment (70°C for 20 min) during the purification of Tba UDG  
661  
662 protein can denature most of *E. coli* proteins (Fig. 1); however, there was a slight  
663  
664 possibility of *E. coli* UDG contamination, which would interfere with our results. To  
665  
666 test this possibility, we used cell extracts made from cells expressing the empty pET-  
667  
668 30a (+) vector. We could detect no cleavage product when using this heated  
669  
670 supernatant produced from the empty vector (data not shown), thus ruling out the  
671  
672 possibility of an *E. coli* UDG contamination during purification of Tba UDG. Overall,  
673  
674 our results suggest that Tba UDG can cleave uracil-containing DNA at high  
675  
676 temperature.  
677  
678  
679  
680

### 681 682 3.2. Biochemical characterization of Tba UDG 683

684 Since *T. barophilus* Ch5 thrives at high temperature (85°C) and we could show  
685  
686 that Tba UDG can cleave uracil-containing DNA at 75°C, we first investigated the  
687  
688 optimal temperature for the enzyme to cleave uracil-containing DNA by using the  
689  
690 uracil-containing ssDNA as the substrate. The cleavage percentage of Tba UDG  
691  
692 increased from 54% to 98% when increasing reaction temperature from 35 to 75°C  
693  
694 (Fig. 2A). Interestingly, even at the lowest tested temperatures, e.g. 35°C and 45°C,  
695  
696 Tba UDG displayed a significant activity, with 54% and 92% cleavage efficiencies  
697  
698  
699  
700 (Fig. 2A), respectively. At the temperatures higher than 75°C, the efficiency  
701  
702  
703  
704  
705  
706  
707  
708

709  
710  
711  
712 decreased to reach 24% at 95°C (Fig. 2A), suggesting that the optimal activity of the  
713  
714 enzyme to cleave uracil-containing ssDNA is between 55°C and 75°C.  
715

716  
717 To further investigate the thermostability of the enzyme, we heated Tba UDG at  
718  
719 various temperatures prior to activity assessments. When heated at 80°C for 30 min,  
720  
721 Tba UDG retained about 90% of cleavage activity (Fig. 2B). The enzyme activity  
722  
723 rapidly decreased at higher temperatures to reach 23% for 85°C and no remaining  
724  
725 activity above 90°C (Fig. 2B). Overall, these observations suggest that Tba UDG is  
726  
727 thermostable.  
728  
729

730  
731 We examined the impact of pH on the endonuclease activity of Tba UDG over a  
732  
733 wide pH range from 4.0 to 11.0 in the standard DNA cleavage reactions. No activity  
734  
735 could be detected at the highest pHs (pH=10 and pH=11, Fig. 2C). By contrast, we  
736  
737 could detect significant cleavage activity even at the lowest pH (pH=4, activity =  
738  
739 69%). The maximal activity was observed for pH ranging from 5 to 8, ranging from  
740  
741 96% to 91%, respectively (Fig. 2C). At pH 9.0, Tba UDG retained 43% cleavage  
742  
743 efficiency. These results suggest that Tba UDG cannot effectively cleave uracil-  
744  
745 containing DNA at high pHs (pH>10.0) and that the optimal pH for this enzyme to  
746  
747 cleave uracil-containing DNA was between 5.0 and 7.0.  
748  
749  
750  
751

752  
753 To evaluate the effects of various divalent metal ions ( $Mg^{2+}$ ,  $Mn^{2+}$ ,  $Ca^{2+}$ ,  $Zn^{2+}$   
754  
755 and  $Cu^{2+}$ ) on the DNA cleavage activity of Tba UDG, we reduced the concentration  
756  
757 of the enzyme in the reactions. In the absence of a divalent ion and in the presence of  
758  
759 EDTA, Tba UDG displayed about 70% cleavage activity (Fig. 2D), suggesting that a  
760  
761 divalent metal ion is not required for the enzyme to cleave uracil-containing DNA.  
762  
763  
764  
765  
766  
767

768  
769  
770  
771 We observed no inhibition of  $\text{Ca}^{2+}$  or  $\text{Mg}^{2+}$  on the activity of Tba UDG, with cleavage  
772 efficiencies ca. 77% in the presence of both ions (Fig. 2D). Two metals, e.g.  $\text{Zn}^{2+}$  or  
773  
774  $\text{Cu}^{2+}$ , were found to totally inhibit the enzyme. Last, the activity of the enzyme was  
775  
776 partially inhibited in the presence of  $\text{Mn}^{2+}$ . Overall, our results suggest that a divalent  
777  
778 metal ion is not needed for Tba UDG to effectively cleave uracil-containing DNA.  
779  
780

781  
782 To uncover the effect of salinity on the Tba UDG activity, we added NaCl with  
783 various concentrations in the DNA cleavage reactions. Under the standard conditions  
784  
785 in the absence of NaCl, Tba UDG cleaved almost completely DNA substrate with  
786  
787 97% of cleavage efficiency (Fig. 2E). No impact of salinity was observed below 200  
788  
789 mM, at which salinity Tba UDG retained 96% of cleavage efficiency, which is similar  
790  
791 to the control reactions (Fig. 2E). However, only 13% cleavage efficiency of Tba  
792  
793 UDG activity was observed in the presence of 400 mM NaCl (Fig. 2E). No cleaved  
794  
795 DNA product was observed at NaCl concentrations from 600 to 1000 mM (Fig. 2E).  
796  
797 These results show that the Tba UDG is a salt-tolerant enzyme, inhibited only by high  
798  
799 NaCl concentrations (>400 mM).  
800  
801

### 802 3.3. *Substrate specificity of Tba UDG*

803  
804

805 To evaluate the substrate specificity of the enzyme, we used the mismatched  
806  
807 DNA (G/T), four mismatched DNA with uracil, and ssDNA with uracil as the  
808  
809 substrates to examine the enzyme activity. As shown in Fig. 3A, the cleavage  
810  
811 efficiencies of Tba UDG were 95%, 88%, 30% and 85% when using the mismatched  
812  
813 DNA with U/G, U/C, U/A and U/T as the substrates, respectively. These results  
814  
815 suggest Tba UDG exhibit various cleavage efficiencies on uracil-containing dsDNA.  
816  
817  
818  
819  
820  
821  
822  
823  
824  
825  
826

827  
828  
829  
830 Furthermore, no cleavage product was found when using mismatched dsDNA (G/T)  
831  
832 (Fig. 3B). The cleavage efficiency of the enzyme was 93% when using uracil-  
833  
834 containing ssDNA as the substrate, which is close to that of using uracil-containg  
835  
836 dsDNA (U/G). Thus, Tba UDG has a preference for substrates with the order from  
837  
838 high to low:  $U \approx U/G > U/T \approx U/C > U/A$ .  
839

#### 840 841 842 *3.4. Kinetics of DNA cleavage by Tba UDG* 843

844 Here, we carried out time course of DNA cleavage activity of Tba UDG under  
845  
846 the optimal reaction condition as described above. As the reaction time extended,  
847  
848 DNA cleavage product of Tba UDG was gradually enhanced until the uracil-  
849  
850 containing ssDNA (Fig. 4A) and dsDNA (Fig. 4B) were almost cleaved. When  
851  
852 reaction time was 10 min, the percent of Tba UDG for cleaving uracil-containing  
853  
854 ssDNA and dsDNA reached 97% and 93%, respectively. These observations suggest  
855  
856 that the enzyme has a strong activity for cleaving uracil-containing DNA at high  
857  
858 temperature.  
859  
860  
861  
862

863 The molar amount of remaining DNA substrate in the DNA cleavage reactions  
864  
865 catalyzed by Tba UDG was plotted as a function of reaction time (Fig. 4C), and the  
866  
867 data were fit to the single-exponential decay equation to yield  $k_{\text{exo}}$ . The  $k_{\text{exo}}$  values  
868  
869 are  $0.25 \pm 0.03 \text{ min}^{-1}$  and  $0.31 \pm 0.04 \text{ min}^{-1}$  for uracil-containing ssDNA and dsDNA,  
870  
871 respectively. Therefore, Tba UDG displays similar rates for cleaving uracil-containing  
872  
873 ssDNA and dsDNA.  
874  
875  
876  
877

#### 878 879 880 *3.5. Mutational analysis of Tba UDG* 881

882 As shown in Fig. 5A, the crystal structure of *S. tokodaii* UDG shows that  
883  
884  
885



886  
887  
888  
889 residues Glu42, His164, Asn82, Phe55 and Glu48 might be key for uracil recognition  
890  
891 [32]. Note that there is no a corresponding amino acid residue in Tba UDG for residue  
892  
893 Glu48 in *S. tokodaii*, and residues Glu42, His164, Asn82 and Phe55 in *S. tokodaii*  
894  
895 UDG correspond to residues Glu118, His216, Asn159 and Tyr127 in Tba UDG.  
896  
897 Sequence comparison shows that these conserved residues Glu118, His216, Asn159  
898  
899 and Tyr127 in Tba UDG are located in Motif B, C, D and F (Fig. 1A), respectively.  
900  
901 To investigate the function of these residues of Tba UDG, we mutated two of these  
902  
903 residues to alanine. The purification profiles of the Tba UDG E118A and N159A  
904  
905 mutants are shown in Fig. 5B.  
906  
907  
908  
909

910  
911 In the control reaction with the wild-type Tba UDG, the enzyme can effectively  
912  
913 cleave the uracil-containing ssDNA (Fig. 6A) and dsDNA (Fig. 6D). When using 500  
914  
915 nM enzyme, the cleavage percent of Tba UDG reached approximate 90%. By  
916  
917 contrast, the E118A and N159A mutants had no cleaving activity, no matter what the  
918  
919 uracil-containing ssDNA or dsDNA was used (Figs. 6B, 6C, 6E and 6F). Therefore,  
920  
921 our data suggest that both mutations enable Tba UDG to abolish its activity, and thus  
922  
923 residues E118 and N159 in the enzyme play essential roles in cleaving uracil-  
924  
925 containing DNA.  
926  
927  
928

### 929 930 *3.6. DNA-binding of the wild-type and mutant Tba UDGs*

931

932  
933 To assess the effect of these two mutations on the affinity of the enzyme to  
934  
935 uracil-containing DNA, we investigated whether or not the wild-type and mutant Tba  
936  
937 UDGs binds to uracil-containing ssDNA or dsDNA by employing EMSA. As shown  
938  
939 in Figs. 7A and 7D, the free uracil-containing ssDNA and dsDNA were gradually  
940  
941  
942  
943  
944

945 bound as increasing the enzyme concentrations. At  $\geq 1,100$  nM Tba UDG, the uracil-  
946 containing ssDNA and dsDNA was almost bound by the enzyme (Figs. 7A and 7D).  
947  
948  
949  
950  
951

952 In contrast, the maximal binding percents of the E118A mutant only reached  
953 35% for uracil-containing ssDNA and 25% for uracil-containing dsDNA even in the  
954 presence of high enzyme concentration (1,500 nM) (Figs. 7B and 7D), suggesting that  
955 the E118A mutant retains the compromised ability to bind to uracil-containing ssDNA  
956 and dsDNA.  
957  
958  
959  
960  
961  
962  
963  
964

965 Compared with the wild-type protein, the N159A mutant displayed the clearly  
966 reduced efficiencies for binding to uracil-containing ssDNA at lower concentration  
967 ( $< 1,100$  nM) (Fig. 7C). However, the binding percent of the N159A mutant was 92%  
968 at 1,500 nM enzyme, which is similar to that of the wild-type protein. On the other  
969 hand, the N159A mutant had the lower efficiency for binding to uracil-containing  
970 dsDNA than the wild-type protein (Fig. 7F). Furthermore, the binding efficiencies of  
971 the N159A mutant were higher than those of the E118A mutant. Thus, the residue  
972 N159 in the Tba UDG is essential for catalysis, and also are involved in binding to  
973 uracil.  
974  
975  
976  
977  
978  
979  
980  
981  
982  
983  
984  
985  
986  
987

#### 988 **4. Discussion**

989 In this work, we characterized biochemically for the first time the thermostable  
990 UDG from the hyperthermophilic archaeon *T. barophilus* Ch5, and revealed that Tba  
991 UDG can specifically cleave uracil-containing DNA at temperatures ranging from 35  
992 to 95°C. Similar to that of the closest homologue, *Pyrococcus furiosus* UDG, the  
993 optimal temperature of the enzyme activity is 55–75°C, which is lower than that of  
994  
995  
996  
997  
998  
999  
1000  
1001  
1002  
1003

1004  
1005  
1006  
1007 the optimal temperature of *T. barophilus* Ch5 [40]. Compared with *A. fulgidus* UDG  
1008  
1009 (80°C) [42], Tba UDG has an slightly lower optimal activity temperature. However,  
1010  
1011 the optimal temperature of Tba UDG activity is clearly higher than that of *S.*  
1012  
1013 *solfataricus* UDG [30], and similar to that of *A. pernix* UDG [29], *P. aerophilum*  
1014  
1015 UDG [41] and *T. maritima* UDG [43]. Thus, the optimal temperatures of archaeal  
1016  
1017 UDGs vary with hyperthermophilic organisms, which might be due to distinct living  
1018  
1019 environments. Furthermore, Tba UDG still retains the pronounced endonuclease  
1020  
1021 activity even when heated at 85°C for 30 min, suggesting that Tba UDG is a  
1022  
1023 thermostable endonuclease. Since the rate of deamination of cytosine increases with  
1024  
1025 temperature, significant amount of uracil might be generated at 85°C, which is the  
1026  
1027 optimal growth temperature of *T. barophilus* Ch5 [40]. Thus, the activity of Tba UDG  
1028  
1029 might be essential for mutation prevention in this organism in response to the known  
1030  
1031 mutagenic potential of uracil.  
1032  
1033  
1034  
1035  
1036  
1037

1038 DNA cleavage efficiencies by UDGs vary with pH. Tba UDG exhibits maximal  
1039  
1040 activity over a broad pH range from 5.0 to 7.0, which is close to that of the purified  
1041  
1042 recombinant *A. fulgidus* UDG that has a optimal pH 4.8 [42]. Interestingly, the native  
1043  
1044 *A. fulgidus* UDG displays maximal activity around pH 6.2 [42]. The difference pHs  
1045  
1046 for optimal activity of *A. fulgidus* UDG from native cells and expression cells might  
1047  
1048 be related to covalent modifications or accessory factors, or a different folding when  
1049  
1050 expressed in the native host. By contrast, the optimal pH for the *A. pernix* UDG  
1051  
1052 activity is estimated to be 8.0 to 10.5, with the highest removal of uracil from ssDNA  
1053  
1054 at pH 9.0 [29]. In addition, the optimal pH for Tba UDG strongly differs from that of  
1055  
1056  
1057  
1058  
1059  
1060  
1061  
1062

1063  
1064  
1065  
1066 its closest homologue, that of *P. furiosus*, which is ca. pH 9 [27]. The rationale for this  
1067  
1068 strong divergences in optimal pHs is quite surprising since most of these Archaea  
1069  
1070 have near neutral intracellular pHs.  
1071

1072  
1073 The reported UDGs are independent on a divalent metal ion [27, 29], which is  
1074  
1075 also the case for Tba UDG. Similar to *A. pernix* UDG [29], Tba UDG is almost  
1076  
1077 inactive to cleave DNA in the presence of Zn<sup>2+</sup> or Cu<sup>2+</sup>. However, both Mg<sup>2+</sup> and  
1078  
1079 Mn<sup>2+</sup> have no detectable effect on DNA cleavage of Tba UDG. However, Mn<sup>2+</sup> shows  
1080  
1081 some inhibition of the activity of *A. pernix* UDG [29].  
1082  
1083

1084  
1085 Tba UDG displays substrate specificity for cleaving DNA in the order:  
1086  
1087 U≈U/G>U/T≈U/C>U/A. By contrast, the *P. furiosus* UDG, as its closest homologue  
1088  
1089 of Tba UDG, removes uracil from various DNA substrates with the following order:  
1090  
1091 U/T≈U/C>U/G≈U/AP≈U/->U/U≈U/I≈U/A [27]. On the other hand, the *A. fulgidus*  
1092  
1093 UDG exhibits opposite base-dependent excision of uracil by the following order:  
1094  
1095 U>U/T>U/C=U/G=U/A [44]. Furthermore, the uracil-releasing activity of *M.*  
1096  
1097 *jannaschii* UDG is observed by the following order U/T>U/C>U/G>U/A [28]. In  
1098  
1099 addition, *A. pernix* UDG exhibits the uracil removal as follows:  
1100  
1101 U/C=U/G>U/T=U/AP=U/->U/U=U/I>U/A [29]. Moreover, *P. aerophilum* UDG  
1102  
1103 shows the substrate specificity by the order: G/U>A/U>ssU [25]. Overall, the  
1104  
1105 substrate specificities of archaeal UDGs vary with these organisms.  
1106  
1107  
1108  
1109  
1110

1111  
1112 On the other hand, Tba UDG has no detected activity on G/T mismatched DNA,  
1113  
1114 similar to *S. solfataricus* UDG [30]. By contrast, the *P. aerophilum* UDG h can cleave  
1115  
1116 normal mismatched DNA (G/T) and U/G [41]. Furthermore, the preferred substrates  
1117  
1118  
1119  
1120  
1121

1122  
1123  
1124  
1125 of *S. solfataricus* UDG and Tba UDG appear to be the G:U-containing double-  
1126  
1127 stranded oligonucleotide. In addition, both Tba UDG and *S. solfataricus* UDG can  
1128  
1129 cleave single-stranded DNA containing uracil; however, Tba UDG displays higher  
1130  
1131 efficiencies for this cleavage than *S. solfataricus* UDG.  
1132  
1133

1134 The uracil recognition mechanisms of several UDGs have been reported,  
1135  
1136 however, an complete understanding on how archaeal UDGs recognize and cleave  
1137  
1138 uracil-containing DNA remains elusive. The crystal structure of *S. tokodaii* UDG  
1139  
1140 suggest that this UDG has a special structure of the leucine-intercalation loop [32],  
1141  
1142 which is distinct from other UDGs, Further mutational analysis on the loop indicates  
1143  
1144 that Tyr170 in *S. tokodaii* UDG is critical for substrate DNA recognition and the  
1145  
1146 catalysis [32]. Mutational studies on the iron sulfur cluster loop motif in the *A.*  
1147  
1148 *fulgidus* uracil-DNA glycosylase suggest that the R86A, C85A and C101A mutants  
1149  
1150 exhibit reduced activity for uracil removal only within double-stranded DNA, while  
1151  
1152 the K100A mutant exhibits enhanced uracil excision activity [45]. In this work, we  
1153  
1154 did the mutational studies based on the *S. tokodaii* UDG structure by mutating  
1155  
1156 residues E118 and N159 in Tba UDG to alanine, which are the corresponding residues  
1157  
1158 E42 and N82 in *S. tokodaii* UDG. Our data show that residues E188 and N159 are key  
1159  
1160 for uracil recognition and removal, suggesting that the conserved motif B and Motif  
1161  
1162 D are important for uracil recognition and removal. Thus, our observations provide  
1163  
1164 new insight into understanding mechanism and function of archaeal UDGs.  
1165  
1166  
1167  
1168  
1169  
1170  
1171  
1172

## 1173 **5. Conclusion**

1174  
1175 In summary, we present the biochemical characteristics and mechanism of the  
1176  
1177  
1178  
1179  
1180

1181  
1182  
1183  
1184 thermostable UDG from *T. barophilus* Ch5 in this work, which is first report on UDG  
1185  
1186 from *Thermococcus* species. The recombinant Tba UDG displays specifically uracil-  
1187  
1188 containing DNA cleavage activity with the highest efficiency at 55–75°C and with an  
1189  
1190 optimal pH of 5.0–7.0. A divalent metal ion is not required for the enzyme to cleave  
1191  
1192 uracil-containing DNA. Furthermore, the enzyme activity is inhibited by Zn<sup>2+</sup> or Cu<sup>2+</sup>,  
1193  
1194 and high NaCl concentration. The enzyme exhibits the substrate specificity by the  
1195  
1196 order: U≈U/G>U/T≈U/C>U/G>U/A. Mutational studies suggest that residues E118  
1197  
1198 and N159 in Tba UDG are essential for uracil recognition and removal. Our work  
1199  
1200 provides a basis for determining the role of Tba UDG in the base excision repair  
1201  
1202 pathway for repairing potentially elevated uracils in *Thermococcus*.  
1203  
1204  
1205  
1206  
1207  
1208  
1209

### 1210 **Acknowledgements**

1211  
1212 This work was supported by the Academic Leader of Middle and Young People  
1213  
1214 of Yangzhou University Grant and Open Project of State Key Laboratory of Microbial  
1215  
1216 Metabolism, Shanghai Jiao Tong University (No. MMLKF18-05) to L.Z.; the practice  
1217  
1218 innovation training program for college students in Yangzhou University to H.S. (No.  
1219  
1220 XKYCX18\_072); Open Project of Key Laboratory of Marine Medicine, Guangdong  
1221  
1222 Province and Key Laboratory of Tropical Marine Bio-resources and Ecology, Chinese  
1223  
1224 Academy of Sciences (2018011008) to L.M.  
1225  
1226  
1227  
1228  
1229

### 1230 **Author contributions**

1240  
1241  
1242  
1243 LZ, ZY and PO designed experiments; HS, QG, HH, HC, YX and LM performed  
1244  
1245 experiments; LZ and PO analyzed data; LZ, ZY and PO wrote and revised the paper.  
1246  
1247

## 1248 **References**

- 1250  
1251  
1252 [1] T. Lindahl, Instability and decay of the primary structure of DNA, *Nature* 362  
1253  
1254 (1993) 709-715.  
1255  
1256 [2] J.C. Shen, W.M. Rideout 3rd, P.A. Jones, The rate of hydrolytic deamination of 5-  
1257  
1258 methylcytosine in double-stranded DNA, *Nucleic Acids Res* 22 (1994) 972-976.  
1259  
1260 [3] T. Lindahl, B. Nyberg, Heat-induced deamination of cytosine residues in  
1261  
1262 deoxyribonucleic acid, *Biochemistry* 13 (1974) 3405-3410.  
1263  
1264 [4] M. Hill-Perkins, M.D. Jones, P. Karran, Site-specific mutagenesis in vivo by  
1265  
1266 single methylated or deaminated purine bases, *Mutat Res* 162 (1986) 153-163.  
1267  
1268 [5] D.W. Grogan, G.T. Carver, J.W. Drake, Genetic fidelity under harsh conditions:  
1269  
1270 analysis of spontaneous mutation in the thermoacidophilic archaeon *Sulfolobus*  
1271  
1272 *acidocaldarius*, *Proc Natl Acad Sci U S A* 98 (2001) 7928-7933.  
1273  
1274 [6] K.L. Jacobs, D.W. Grogan, Rates of spontaneous mutation in an archaeon from  
1275  
1276 geothermal environments, *J Bacteriol* 179 (1997) 3298-3303.  
1277  
1278 [7] A. Koulis, D.A. Cowan, L.H. Pearl, R. Savva, Uracil-DNA glycosylase activities  
1279  
1280 in hyperthermophilic micro-organisms, *FEMS Microbiol Lett* 143 (1996) 267-  
1281  
1282 271.  
1283  
1284 [8] S.S. Wallace, Base excision repair: a critical player in many games, *DNA Repair*  
1285  
1286 (Amst) 19 (2014) 14-26.  
1287  
1288  
1289  
1290  
1291  
1292  
1293  
1294  
1295  
1296  
1297  
1298

- 1299  
1300  
1301  
1302 [9] N. Schormann, R. Ricciardi, D. Chattopadhyay, Uracil-DNA glycosylases-  
1303  
1304 Structural and functional perspectives on an essential family of DNA repair  
1305  
1306 enzymes, *Protein Sci* 23 (2014) 1667-1685.  
1307  
1308  
1309 [10] C.D. Mol, A.S. Arvai, G. Slupphaug, B. Kavli, I. Alseth, H.E. Krokan, J.A.  
1310  
1311 Tainer, Crystal structure and mutational analysis of human uracil-DNA  
1312  
1313 glycosylase: structural basis for specificity and catalysis, *Cell* 80 (1995) 869-878.  
1314  
1315  
1316 [11] S.S. Parikh, C.D. Putnam, J.A. Tainer, Lessons learned from structural results on  
1317  
1318 uracil-DNA glycosylase, *Mutat Res* (2000) 183-199.  
1319  
1320  
1321 [12] L.H. Pearl, Structure and function in the uracil-DNA glycosylase superfamily,  
1322  
1323 *Mutat Res* (2000) 165-181.  
1324  
1325  
1326 [13] R. Savva, K. McAuley-Hecht, T. Brown, L. Pearl, The structural basis of specific  
1327  
1328 base-excision repair by uracil-DNA glycosylase, *Nature* (1995) 487-493.  
1329  
1330  
1331 [14] G. Slupphaug, C.D. Mol, B. Kavli, A.S. Arvai, H.E. Krokan, J.A. Tainer, A  
1332  
1333 nucleotide-flipping mechanism from the structure of human uracil-DNA  
1334  
1335 glycosylase bound to DNA, *Nature* 384 (1996) 87-92.  
1336  
1337  
1338 [15] G.Y. Xiao, M. Tordova, J. Jagadeesh, A.C. Drohat, J.T. Stivers, G.L. Gilliland,  
1339  
1340 Crystal structure of *Escherichia coli* uracil DNA glycosylase and its complexes  
1341  
1342 with uracil and glycerol: Structure and glycosylase mechanism revisited, *Proteins*  
1343  
1344 35 (1999) 13-24.  
1345  
1346  
1347 [16] T.E. Barrett, R. Savva, G. Panayotou, T. Barlow, T. Brown, J. Jiricny, L.H. Pearl,  
1348  
1349 Crystal structure of a G:T/U mismatch-specific DNA glycosylase: mismatch  
1350  
1351 recognition by complementary-strand interactions, *Cell* 92 (1998) 117-129.  
1352  
1353  
1354  
1355  
1356  
1357



- 1358  
1359  
1360  
1361 [17] K.A. Haushalter, M.W. Todd Stukenberg, M.W. Kirschner, G.L. Verdine,  
1362  
1363 Identification of a new uracil-DNA glycosylase family by expression cloning  
1364  
1365 using synthetic inhibitors, *Curr Biol* 9 (1999) 174-185.  
1366  
1367  
1368 [18] J.A. Hinks, M.C. Evans, Y. De Miguel, A.A. Sartori, J. Jiricny, L.H. Pearl, An  
1369  
1370 iron-sulfur cluster in the family 4 uracil-DNA glycosylases, *J Biol Chem* 277  
1371  
1372 (2002) 16936-16940.  
1373  
1374  
1375 [19] J. Hoseki, A. Okamoto, R. Masui, T. Shibata, Y. Inoue, S. Yokoyama, S.  
1376  
1377 Kuramitsu, Crystal structure of a family 4 uracil-DNA glycosylase from *Thermus*  
1378  
1379 *thermophilus* HB8, *J Mol Biol* 333 (2003) 515-526.  
1380  
1381  
1382 [20] V. Starkuviene, H.J. Fritz, A novel type of uracil-DNA glycosylase mediating  
1383  
1384 repair of hydrolytic DNA damage in the extremely thermophilic eubacterium  
1385  
1386 *Thermus thermophilus*, *Nucleic Acids Res* 30 (2002) 2097-2102.  
1387  
1388  
1389 [21] H. Kosaka, J. Hoseki, N. Nakagawa, S. Kuramitsu, R. Masui, Crystal structure of  
1390  
1391 family 5 uracil-DNA glycosylase bound to DNA, *J Mol Biol* 373 (2007) 839-  
1392  
1393 850.  
1394  
1395  
1396 [22] A.A. Sartori, S. Fitz-Gibbon, H. Yang, J.H. Miller, J. Jiricny, A novel uracil-  
1397  
1398 DNA glycosylase with broad substrate specificity and an unusual active site,  
1399  
1400 *EMBO J* 21 (2002) 3182-3191.  
1401  
1402  
1403 [23] H.W. Lee, B.N. Dominy, W. Cao, New family of deamination repair enzymes in  
1404  
1405 uracil-DNA glycosylase superfamily, *J Biol Chem* 286 (2011) 31282-31287.  
1406  
1407  
1408 [24] M. Sandigursky, W.A. Franklin, Uracil-DNA glycosylase in the extreme  
1409  
1410 thermophile *Archaeoglobus fulgidus*, *J Biol Chem* 275 (2000) 19146-19149.  
1411  
1412  
1413  
1414  
1415  
1416

- 1417  
1418  
1419  
1420 [25] A.A. Sartori, P. Schar, S. Fitz-Gibbon, J.H. Miller, J. Jiricny, Biochemical  
1421  
1422 characterization of uracil processing activities in the hyperthermophilic archaeon  
1423  
1424 *Pyrobaculum aerophilum*, J Biol Chem 276 (2001) 29979-29986.  
1425  
1426  
1427 [26] S. Kiyonari, M. Uchimura, T. Shirai, Y. Ishino, Physical and functional  
1428  
1429 interactions between uracil-DNA glycosylase and proliferating cell nuclear  
1430  
1431 antigen from the euryarchaeon *Pyrococcus furiosus*, J Biol Chem 283 (2008)  
1432  
1433 24185-24193.  
1434  
1435  
1436 [27] L.B. Lin, Y.F. Liu, X.P. Liu, J.H. Liu, Biochemical characterization of uracil-  
1437  
1438 DNA glycosylase from *Pyrococcus furiosus*, Chem Res Chinese U 28 (2012)  
1439  
1440 477-482.  
1441  
1442  
1443 [28] J.H. Chung, E.K. Im, H.Y. Park, J.H. Kwon, S. Lee, J. Oh, K.C. Hwang, J.H.  
1444  
1445 Lee, Y. Jang, A novel uracil-DNA glycosylase family related to the helix-  
1446  
1447 hairpin-helix DNA glycosylase superfamily, Nucleic Acids Res 31 (2003) 2045-  
1448  
1449 2055.  
1450  
1451  
1452 [29] X.P. Liu, J.H. Liu, Characterization of family IV UDG from *Aeropyrum pernix*  
1453  
1454 and its application in hot-start PCR by family B DNA polymerase, PLoS One 6  
1455  
1456 (2011) e27248.  
1457  
1458  
1459 [30] I. Dionne, S.D. Bell, Characterization of an archaeal family 4 uracil DNA  
1460  
1461 glycosylase and its interaction with PCNA and chromatin proteins, Biochem J  
1462  
1463 387 (2005) 859-863.  
1464  
1465  
1466 [31] A. Kawai, S. Higuchi, M. Tsunoda, K.T. Nakamura, S. Miyamoto, Purification,  
1467  
1468 crystallization and preliminary X-ray analysis of uracil-DNA glycosylase from  
1469  
1470  
1471  
1472  
1473  
1474  
1475

- 1476  
1477  
1478  
1479 *Sulfolobus tokodaii* strain 7, Acta Crystallogr F 68 (2012) 1102-1105.  
1480  
1481 [32] A. Kawai, S. Higuchi, M. Tsunoda, K.T. Nakamura, Y. Yamagata, S. Miyamoto,  
1482  
1483 Crystal structure of family 4 uracil-DNA glycosylase from *Sulfolobus tokodaii*  
1484  
1485 and a function of tyrosine 170 in DNA binding, FEBS Lett 589 (2015) 2675-  
1486  
1487 2682.  
1488  
1489  
1490 [33] G.S. Yi, W.W. Wang, W.G. Cao, F.P. Wang, X.P. Liu, *Sulfolobus*  
1491  
1492 *acidocaldarius* UDG can remove dU from the RNA backbone: insight into the  
1493  
1494 specific recognition of uracil linked with deoxyribose, Genes (Basel) 8 (2017)  
1495  
1496 E38.  
1497  
1498  
1499 [34] M.N. Moen, I. Knaevelsrud, G.T. Haugland, K. Grosvik, N.K. Birkeland, A.  
1500  
1501 Klungland, S. Bjelland, Uracil-DNA glycosylase of *Thermoplasma acidophilum*  
1502  
1503 directs long-patch base excision repair, which is promoted by deoxynucleoside  
1504  
1505 triphosphates and ATP/ADP, into short-patch repair, J Bacteriol 193 (2011)  
1506  
1507 4495-4508.  
1508  
1509  
1510 [35] H. Yang, J.H. Chiang, S. Fitz-Gibbon, M. Lebel, A.A. Sartori, J. Jiricny, M.M.  
1511  
1512 Slupska, J.H. Miller, Direct interaction between uracil-DNA glycosylase and a  
1513  
1514 proliferating cell nuclear antigen homolog in the crenarchaeon *Pyrobaculum*  
1515  
1516 *aerophilum*, J Biol Chem 277 (2002) 22271-22278.  
1517  
1518  
1519 [36] G.L. Moldovan, B. Pfander, S. Jentsch, PCNA, the maestro of the replication  
1520  
1521 fork, Cell 129 (2007) 665-679.  
1522  
1523  
1524 [37] M. van Wolferen, M. Ajon, A.J.M. Driessen, S.V. Albers, How  
1525  
1526 hyperthermophiles adapt to change their lives: DNA exchange in extreme  
1527  
1528  
1529  
1530  
1531  
1532  
1533  
1534

- 1535  
1536  
1537  
1538 conditions, *Extremophiles* 17 (2013) 545-563.  
1539
- 1540 [38] Y.J. Kim, H.S. Lee, E.S. Kim, S.S. Bae, J.K. Lim, R. Matsumi, A.V. Lebedinsky,  
1541  
1542 T.G. Sokolova, D.A. Kozhevnikova, S.S. Cha, S.J. Kim, K.K. Kwon, T.  
1543 Imanaka, H. Atomi, E.A. Bonch-Osmolovskaya, J.H. Lee, S.G. Kang, Formate-  
1544  
1545 driven growth coupled with H<sub>2</sub> production, *Nature* 467 (2010) 352-355.  
1546  
1547  
1548  
1549
- 1550 [39] V.T. Marteinsson, J.L. Birrien, A.L. Reysenbach, M. Vernet, D. Marie, A.  
1551  
1552 Gambacorta, P. Messner, U.B. Sleytr, D. Prieur, *Thermococcus barophilus* sp.  
1553  
1554 nov., a new barophilic and hyperthermophilic archaeon isolated under high  
1555  
1556 hydrostatic pressure from a deep-sea hydrothermal vent, *Int J Syst Bacteriol* 49  
1557  
1558 (1999) 351-359.  
1559
- 1560 [40] P. Oger, T.G. Sokolova, D.A. Kozhevnikova, E.A. Taranov, P. Vannier, H.S.  
1561  
1562 Lee, K.K. Kwon, S.G. Kang, J.H. Lee, E.A. Bonch-Osmolovskaya, A.V.  
1563  
1564 Lebedinsky, Complete genome sequence of the hyperthermophilic and  
1565  
1566 piezophilic archaeon *Thermococcus barophilus* Ch5, capable of growth at the  
1567  
1568 expense of hydrogenogenesis from carbon monoxide and formate, *Genome*  
1569  
1570 *Announc* 4 (2016).  
1571  
1572  
1573  
1574  
1575
- 1576 [41] H. Yang, S. Fitz-Gibbon, E.M. Marcotte, J.H. Tai, E.C. Hyman, J.H. Miller,  
1577  
1578  
1579 Characterization of a thermostable DNA glycosylase specific for U/G and T/G  
1580  
1581 mismatches from the hyperthermophilic archaeon *Pyrobaculum aerophilum*, *J*  
1582  
1583 *Bacteriol* 182 (2000) 1272-1279.  
1584  
1585
- 1586 [42] I. Knaevelsrud, S. Kazazic, N.K. Birkeland, S. Bjelland, The pH optimum of  
1587  
1588 native uracil-DNA glycosylase of *Archaeoglobus fulgidus* compared to  
1589  
1590  
1591  
1592  
1593

1594  
1595  
1596  
1597 recombinant enzyme indicates adaption to cytosolic pH, *Acta Biochim Pol* 61  
1598  
1599 (2014) 393-395.  
1600

1601  
1602 [43] M. Sandigursky, A. Faje, W.A. Franklin, Characterization of the full length  
1603 uracil-DNA glycosylase in the extreme thermophile *Thermotoga maritima*,  
1604  
1605 *Mutat Res* 485 (2001) 187-195.  
1606  
1607

1608  
1609 [44] I. Knaevelsrud, P. Ruoff, H. Anensen, A. Klungland, S. Bjelland, N.K.  
1610 Birkeland, Excision of uracil from DNA by the hyperthermophilic Afung protein  
1611 is dependent on the opposite base and stimulated by heat-induced transition to a  
1612 more open structure, *Mutat Res* 487 (2001) 173-190.  
1613  
1614  
1615  
1616  
1617

1618  
1619 [45] L.M. Engstrom, O.A. Partington, S.S. David, An iron-sulfur cluster loop motif in  
1620 the *Archaeoglobus fulgidus* uracil-DNA glycosylase mediates efficient uracil  
1621 recognition and removal, *Biochemistry* 51 (2012) 5187-5197.  
1622  
1623  
1624  
1625  
1626  
1627  
1628  
1629  
1630  
1631  
1632  
1633  
1634  
1635  
1636  
1637  
1638  
1639  
1640  
1641  
1642  
1643  
1644  
1645  
1646  
1647  
1648  
1649  
1650  
1651  
1652

## Figure legends

**Fig. 1.** Tba UDG can cleave uracil-containing ssDNA and dsDNA at high temperature. A. Partial amino acid alignment of UDGs from hyperthermophilic crenarchaea, euryarchaea and bacteria. Tba: *Thermococcus barophilus* (WP\_056934618.1); Pfu: *Pyrococcus furiosus* (WP\_011012532.1); Pho: *Pyrococcus horikoshii* (WP\_048053599.1); Afu: *Archaeoglobus fulgidus* (GenBank: AIG99287.1); Pae: *Pyrobaculum aerophilum* (GenBank: AAL62921.1); Ape: *Aeropyrum pernix* (GenBank: BAA79385.2); Sso: *Sulfolobus solfataricus* (GenBank: AKA78326.1); Sto: *Sulfolobus tokodaii* (PDB: 4ZBY); Tma: *Thermotoga maritima* (PDB: 1L9G\_A). B. The conserved Motif B and Motif F in six families of UDG. Family 1, Eco (*E. coli*) UDG (EMBL:J03725); Family 2, Human TDG (EMBL:U51166); Family 3, Human SUMG1 (EMBL: AF125182); Family 4, Tba UDG247 (NCBI reference sequence: WP\_056934618.1); Family 5, *P. aerophilum* (Pae) UDGb (NP\_559226); Family 6, Mba (*Methanosarcina barkeri*) HDG (YP\_304295.1). C. Overexpression and purification of Tba UDG. M: Protein marker. D. DNA cleavage assays of Tba UDG. DNA cleavage reactions were performed by Tba UDG in the presence of normal and uracil-containing ssDNA and dsDNA at 65°C. CK: the reaction without the enzyme.

**Fig. 2.** Biochemical characterization of Tba UDG. A. The optimal temperature of the enzyme. B. The thermostability of the enzyme. C. The pH adaptation of the enzyme. D. Effects of divalent metal ions on the enzyme activity. E. Effect of NaCl on the enzyme activity. Reaction products were detected by electrophoresis through running

1712  
1713  
1714  
1715 a 15% denaturing PAGE. CK: the reaction without the enzyme; CK1 in the panel B:  
1716  
1717 the reaction without the enzyme; CK2 in the panle B: the reaction with the unheated  
1718  
1719 enzyme.  
1720

1721  
1722  
1723 **Fig. 3.** Substrate specificity of Tba UDG. DNA cleavage reactions of Tba UDG were  
1724 performed using the uracil-containing ssDNA and dsDNA, and mismatched DNA  
1725 (G/T) as the substrates. Reaction products were analyzed by electrophoresis through  
1726 running a 15% denaturing PAGE. A. The substrates were ssDNA with U, and  
1727 mismatched dsDNA with U/T, U/C, U/G, or U/A. B. The substrates were mismatched  
1728 DNA (G/T). CK: the reaction without the enzyme.  
1729  
1730  
1731  
1732  
1733  
1734  
1735  
1736  
1737

1738  
1739 **Fig. 4.** Kinetic analysis of DNA cleavage of Tba UDG. DNA cleavage reactions by  
1740 Tba UDG were performed under the optimal reaction condition at various time (10  
1741 sec – 30 min). Reaction products were analyzed by electrophoresis through running a  
1742 12% denaturing PAGE. A. Uracil-containing ss DNA cleavage; B. Uracil-containing  
1743 ds DNA cleavage. CK: the reaction without the enzyme; C. Rate of DNA cleavage  
1744 catalyzed by Tba UDG. By using the single-exponential decay equation, the amount  
1745 of remaining substrate was plotted as a function of time to yeild the best fit (the solid  
1746 lines). Tba UDG cleaved the uracil-containing ssDNA ( $\circ$ ) and dsDNA ( $\square$ ) at the rates  
1747 of  $0.25 \pm 0.03 \text{ min}^{-1}$  and  $0.31 \pm 0.04 \text{ min}^{-1}$ , respectively.  
1748  
1749  
1750  
1751  
1752  
1753  
1754  
1755  
1756  
1757  
1758  
1759

1760  
1761 **Fig. 5.** Possible uracil recognition mechanism of Tba UDG. A. Interactions between  
1762 amino acid residues and uracil of Tba UDG. The residues E42, N82, H164 and F55 in  
1763 *S. tokodaii* UDG that correspond to the residues E118, N159, H216 and Y127 in Tba  
1764  
1765  
1766  
1767  
1768  
1769  
1770

1771  
1772  
1773  
1774 UDG are depicted in blue, red, cyan and yellow sticks, respectively. The figure was  
1775  
1776 adapted from the *S. tokodaii* UDG structure (PDB: 4zby) by Pymol [32]. Tba UDG  
1777  
1778 residues are indicated in parentheses. The uracil is shown with dots. B. Purification of  
1779  
1780 the wild-type, E118A and N159A Tba UDG mutant proteins. M: Protein marker.

1783  
1784 **Fig. 6.** DNA cleavage assays of the wild-type and mutant Tba UDGs. DNA cleavage  
1785  
1786 reactions of Tba UDG were performed using uracil-containing ssDNA and dsDNA as  
1787  
1788 the substrates at 65°C for 10 min, respectively. Reaction products were analyzed by  
1789  
1790 electrophoresis through running a 15% denaturing PAGE. A. Cleaving uracil-  
1791  
1792 containing ssDNA by the wild-type; B. Cleaving uracil-containing ssDNA by the  
1793  
1794 E118A mutant; C. Cleaving uracil-containing ssDNA by the N159A mutant; D.  
1795  
1796 Cleaving uracil-containing dsDNA by the wild type; E. Cleaving uracil-containing  
1797  
1798 dsDNA by the E118A mutant; F. Cleaving uracil-containing dsDNA by the N159A  
1799  
1800 mutant. CK: the reaction without the enzyme.

1801  
1802 **Fig. 7.** The binding assays of the wild-type and mutant Tba UDGs. The uracil-  
1803  
1804 containing ssDNA and dsDNA (U:G) were employed as the substrates to examine the  
1805  
1806 DNA-binding of the wild-type and mutant Tba UDGs. The wild-type and mutant Tba  
1807  
1808 UDGs and DNA were incubated at 25°C for 10 min, and were run by electrophoresis  
1809  
1810 on a 4% native polyacrylamide gel. A. Binding to uracil-containing ssDNA by the  
1811  
1812 wild-type protein; B. Binding to uracil-containing ssDNA by the E118A mutant; C.  
1813  
1814 Binding to uracil-containing ssDNA by the N159A mutant; D. Binding to uracil-  
1815  
1816 containing dsDNA by the wild-type protein; E. Binding to uracil-containing dsDNA



1830  
1831  
1832  
1833  
1834  
1835  
1836  
1837  
1838  
1839  
1840  
1841  
1842  
1843  
1844  
1845  
1846  
1847  
1848  
1849  
1850  
1851  
1852  
1853  
1854  
1855  
1856  
1857  
1858  
1859  
1860  
1861  
1862  
1863  
1864  
1865  
1866  
1867  
1868  
1869  
1870  
1871  
1872  
1873  
1874  
1875  
1876  
1877  
1878  
1879  
1880  
1881  
1882  
1883  
1884  
1885  
1886  
1887  
1888

by the E118A mutant; F. Binding to uracil-containing dsDNA by the N159A mutant.

CK: the binding assay without the enzyme.

**Table 1** Sequences of the oligonucleotides used to clone the Tba UDG gene and construct its mutants

Name	Sequence (5'-3')
Tba UDG F	GGAATTCC <i>ATATGCTGCTGGAGTTTGAACGCC</i>
Tba UDG R	CCGCTCGAGTTTAGTAATATTTAAGCTTTTCC
E118A F	AAAGGTTGTTTTGGTCGGGG <u>GCGG</u> CTCCAGGAAGGAAAGGCT
E118A R	AGCCTTTCCTTCCTGGAGCC <u>GCC</u> CCCGACCAAACAACCTTT
N159A F	TTTTGTGTATATCACAG <u>CT</u> GTTGTAAAATGCAATC
N159A R	<u>AGCT</u> GTGATATACACAAAATCGGGGTTAATTCCGA

The italic nucleotides represent restriction sites.

The substitution bases are underlined.

1948  
1949  
1950  
1951  
1952  
1953  
1954  
1955  
1956  
1957  
1958  
1959  
1960  
1961  
1962  
1963  
1964  
1965  
1966  
1967  
1968  
1969  
1970  
1971  
1972  
1973  
1974  
1975  
1976  
1977  
1978  
1979  
1980  
1981  
1982  
1983  
1984  
1985  
1986  
1987  
1988  
1989  
1990  
1991  
1992  
1993  
1994  
1995  
1996  
1997  
1998  
1999  
2000  
2001  
2002  
2003  
2004  
2005  
2006

**Table 2** Sequences of the oligonucleotides used in this work

Number	Sequence (5'-3')
1	CGAACTGCCTGGAATCCTGACGAC <u>U</u> TGTAGCGAACGATCACCTCA
2	CGAACTGCCTGGAATCCTGACGAC <u>C</u> TGTAGCGAACGATCACCTCA
3	CGAACTGCCTGGAATCCTGACGAC <u>G</u> TGTAGCGAACGATCACCTCA
4	TGAGGTGATCGTTCGCTACAG <u>G</u> TCGTCAGGATTCCAGGCAGTTCG
5	TGAGGTGATCGTTCGCTACAC <u>G</u> TCGTCAGGATTCCAGGCAGTTCG
6	TGAGGTGATCGTTCGCTACA <u>A</u> GTCGTCAGGATTCCAGGCAGTTCG
7	TGAGGTGATCGTTCGCTACA <u>I</u> GTCGTCAGGATTCCAGGCAGTTCG

The underlined base is used to prepare normal and uracil-containing dsDNA.

**Table 3** DNA substrates prepared with the oligonucleotides in Table 2

Strand	labeling	Combination	Base pair
ssDNA	Cy3	1*	U/-
ssDNA	Cy3	2*	C/-
dsDNA	Cy3	1*+4	U/G
dsDNA	Cy3	1*+5	U/C
dsDNA	Cy3	1*+6	U/A
dsDNA	Cy3	1*+7	U/T
dsDNA	Cy3	2*+4	C/G
dsDNA	Cy3	3*+6	G/T

The symbol “\*” indicates the labeled strand.

**A**

		<u>Motif A</u>	<u>Motif B</u>	<u>Motif C</u>		<u>Motif D</u>
Tba	101	GLPFANGVWGSKVVLVGEAP	G---RKGCYTG	ICFYRDASGMLLRKALFSL	-GINPD-----	FVYITNVVKCNPPENKLGVD--KREL
Pfu	29	PVP-GYGNDAKIMFVGEAP	GYWEDQKGLPFVG	-----KAGKVLDELDDGI	-GLTRE-----	DVYITNVVKCRPPNRRDPTEEEIKACS
Pho	23	PVP-GDGSYDTRKIMFVGEAP	GYWEDQMGLPFVG	-----KAGKVLDELKLI	-GLKRS-----	EVYITNIVKCRPPNRRDPTEEEIKACA
Afu	26	YVP-GVGNKAEIVFVGEAP	GRDEDLKGEPFVG	-----AAGKLLTEMLASI	-GLRRE-----	DVYITNVVKCRPPNRRDPTEEEVEKCG
Pae	25	AVP-GEGMKLGMIVVGEAP	GASEDEAGRPFVG	-----AAGQLLTEALSRL	-GVRRG-----	DVFTITNVVKCRPPNRRTPNREEVEACL
Ape	28	AVP-GEGPGEAGVMVGEAP	GRMEDRLGRPFVG	-----PAGKLLDLSLELA	-GLSRG-----	EVYITNVVKCRPPGNRRDPREEIEACL
Sso	32	PVP-PNGQIDAEIVIVGLAP	AGNGGNRTGRMFTGD	-----ESSNNLANALYAV	-GLSNQPFVSKDDGLKLF	NVYITSAVKCAPPNK-PNKDEIINCS
Sto	30	GYP-----KAEIMFVGEAP	GENEDKGRPFVG	-----AAGKLLTQMIKEIL	GLERD-----	QVFTITNVVKCRPPNRRDPPEDEITACS
Tma	30	VVV-GEGNLDTRIVFVGEAP	GEEEDKTGRPFVG	-----RAGMLLTELRES	-GIRRE-----	DVYICNVVKCRPPNRRTPTEEQACG

Motif E

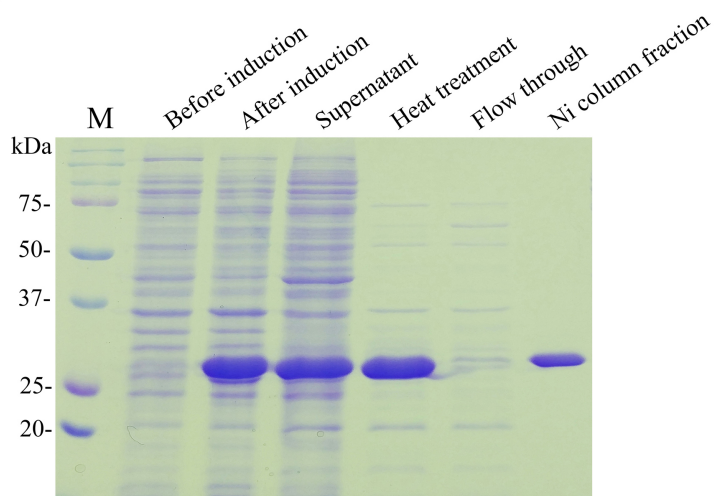
Motif F

Tba	179	SLLKKELEIFR	-PKAIFALGR	----	TAEKALKRVGFDA	-----	VYLR*	HPAWYVRRGLREPNDMLEEY									
Pfu	106	PYLDQQIDIIK	-PKVIVTLGR	----	HSTNYILKKFGFDLEPISKIH	GKVFKA	TLFGTLY	-IFPT	YHPAVALYRP--QLKEELKQDF								
Pho	100	PYLDQQIDIIK	-PKVIVTLGR	----	FSTAYIMKKYGFNVEPISKIH	GRVFEARTLFGKIY	-IVPM	YHPAVALYRP--QLRRELEEDF									
Afu	103	NYLVRQLEAIR	-PNVIVCLGR	----	FAAQFIENLFDLEFTTISR	VKGKVEVERW	GKVKV	-VIAI	YHPAVALYRP--QLREEYESDF								
Pae	102	PYLTIQQIGILK	-PRRIIALGL	----	ISAKALMELMGRRAEKLGDV	VKGKCYQGR	IAGVQVE	-LCIT	YHPAVALRKP--ALRGEFQKDL								
Ape	105	PYLVEQISLIR	-PRLVIAVGR	----	HAGRTLFRLAGLRWPLARARG	RVWRGRIGGV	ELL	-IAVT	YHPAALYNP--GLRGELEDF								
Sso	123	VFLVEEVRIKNTKVI	IALGRIAWDSL	LIYVFKK	IGYNVNPVRFYH	GALVKKV	KPDMS	I	IWL	VGS	YHPS	PRNMKTG	-RLT	INMLIEI			
Sto	104	PYLDQQIDIIIM	-PKIIVTLGR	----	HSTKYIFSKMGENFSSITK	VRGKSYVWKY	KEKE	-I	IVFPT	YHPAALYNPN--LRKILEEDF							
Tma	107	HFLLAQIEIIN	-PDVIVALGA	----	TALSFFV	---	DGKKV	SITK	VRGNPID	--	WLG	GK	KV	-I	-PT	FHPSYLLRNR	SNELRRIVLEDI

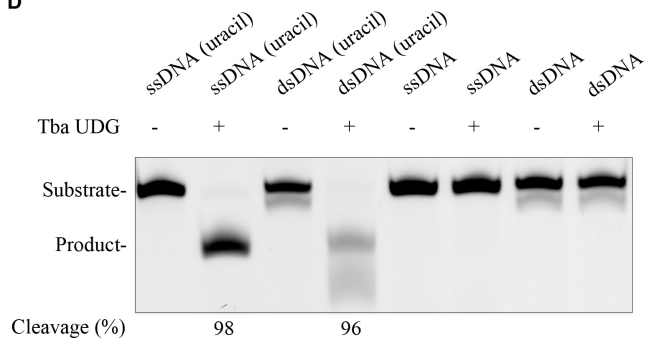
**B**

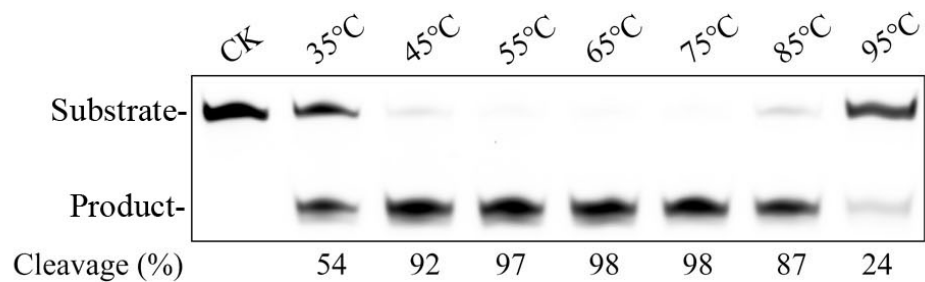
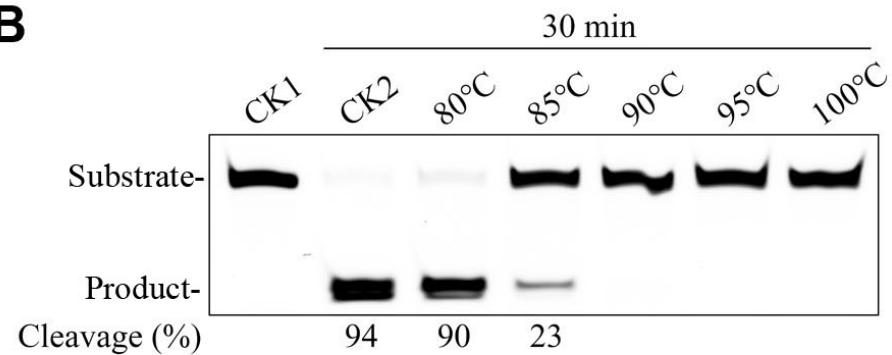
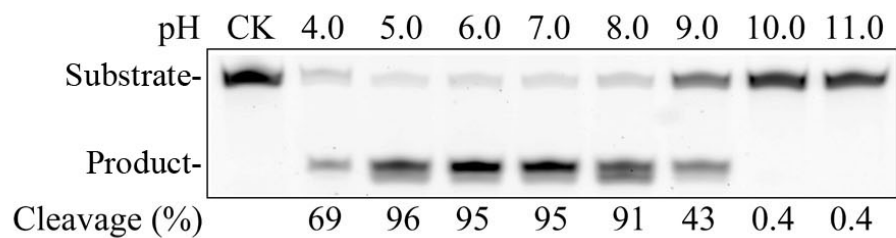
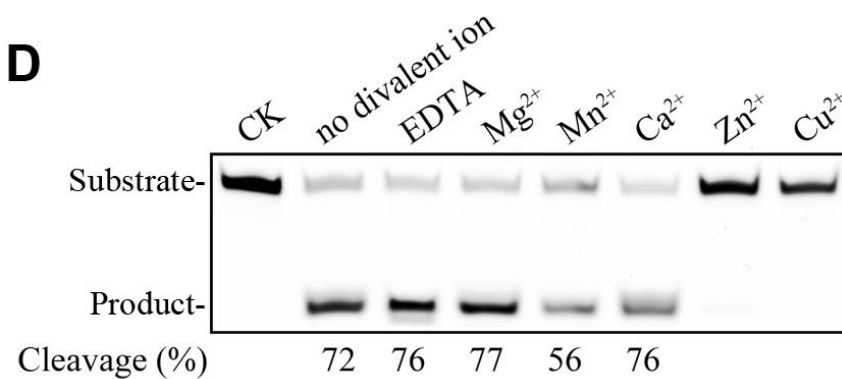
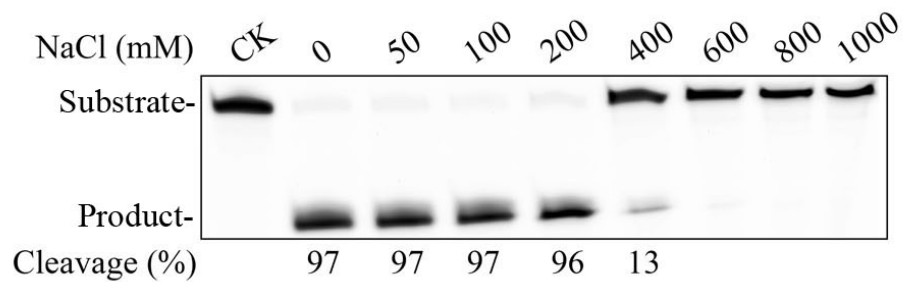
			<u>Motif B</u>		<u>Motif F</u>	
Family 4	Tba	UDG	113	V V L V G E A P G	216	H P A W Y V R
Family 1	Eco	UDG	58	V V I L G Q D P Y	187	H P S P L S A
Family 2	Human	TDG	134	I V I I G I N P G	269	M P S S S A R
Family 3	Human	SMUG1	79	V L F L G M N P G	239	H P S P R N P
Family 5	Pae	UDGb	62	V M V V G L A P G	196	H P S P L N V
Family 6	Mba	HDG	42	W R L L G S I I G	136	S S S G A N R

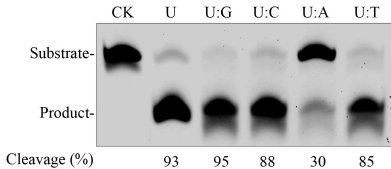
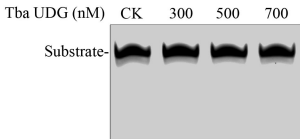
**C**

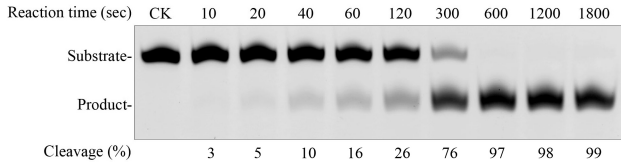
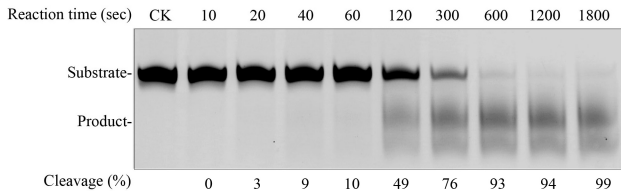
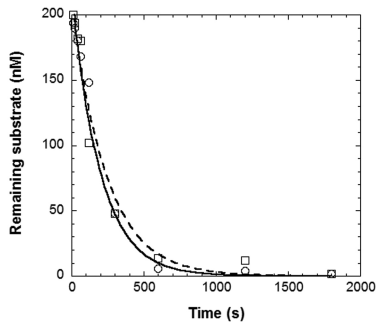


**D**

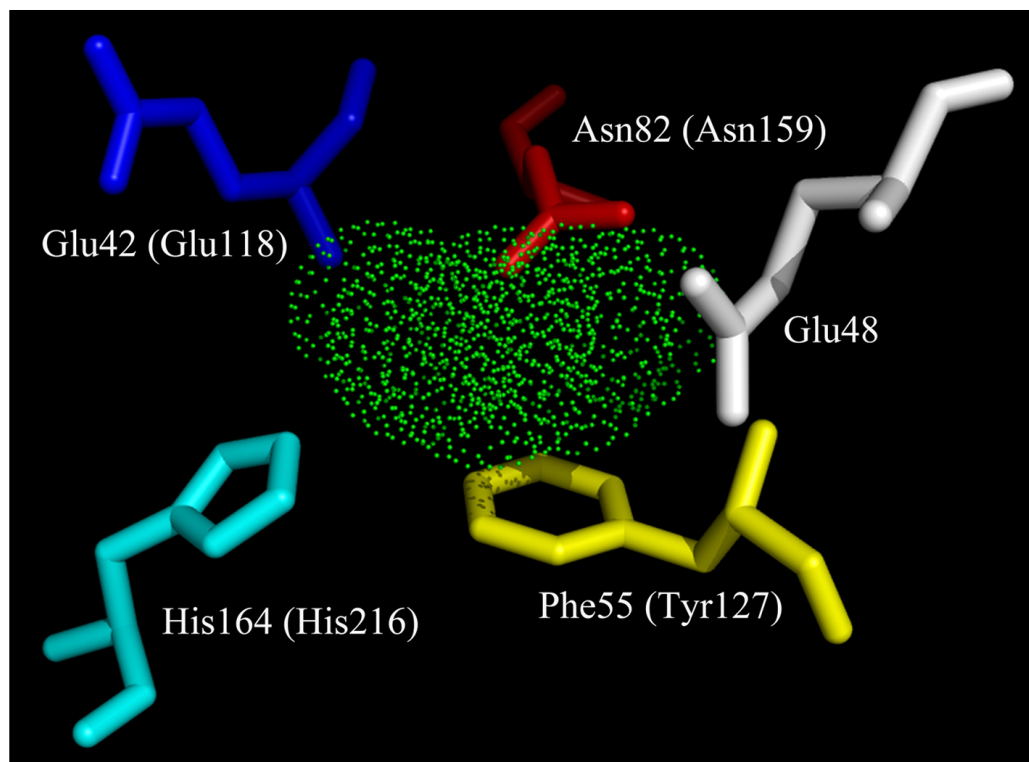
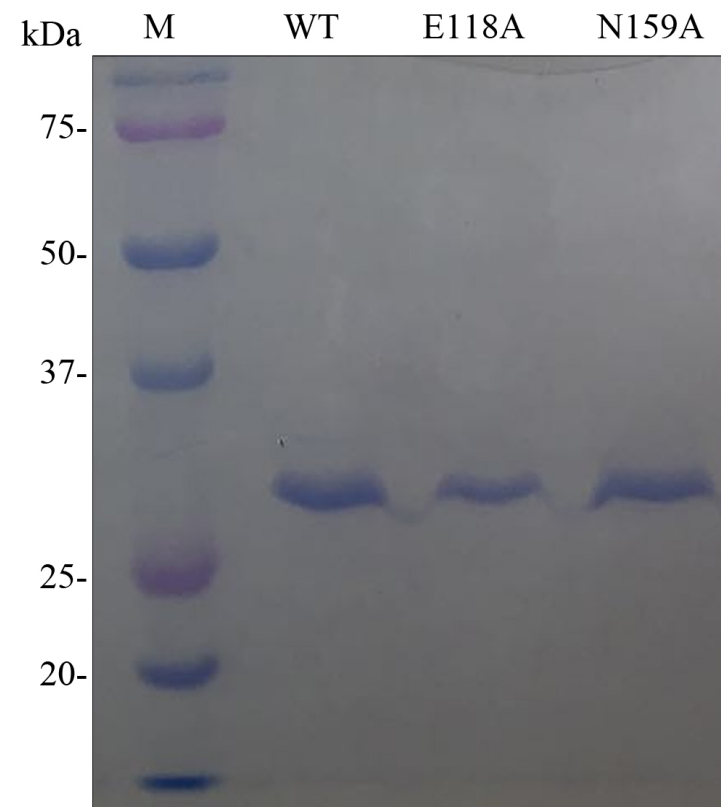


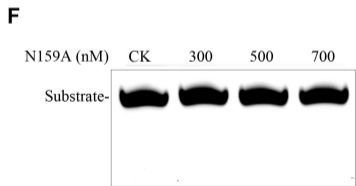
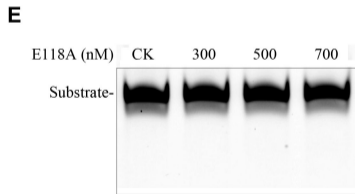
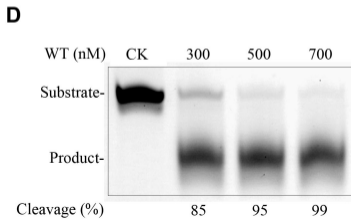
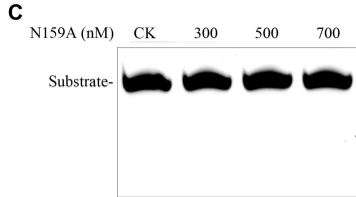
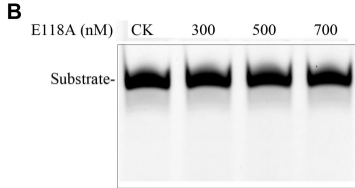
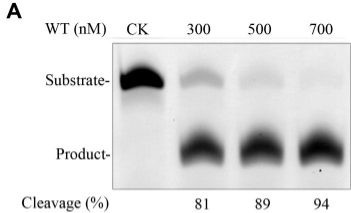
**A****B****C****D****E**

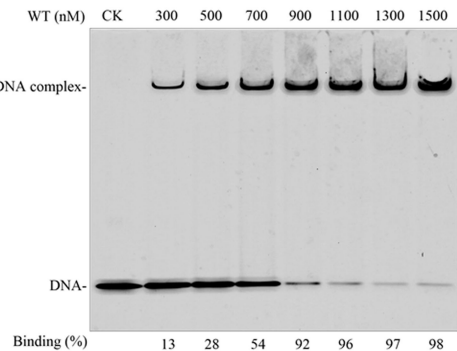
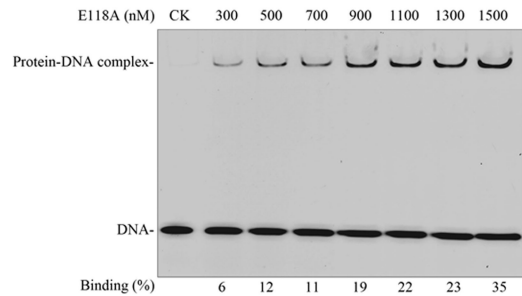
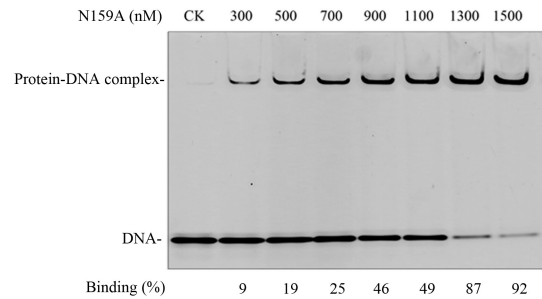
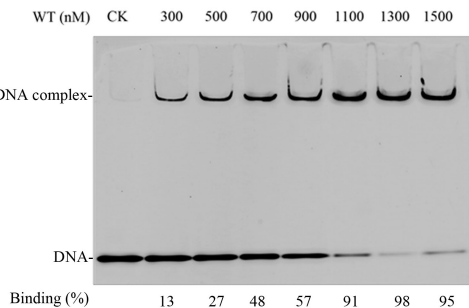
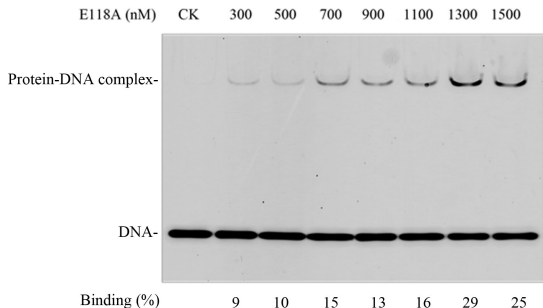
**A****B**

**A****B****C**



**A****B**



**A****B****C****D****E****F**